Available online at www.sciencedirect.com

ScienceDirect

Ceramics International 40 (2014) 2793–2798

CERAMICS INTERNATIONAL

www.elsevier.com/locate/ceramint

Effects of copper on microstructure and mechanical properties of C_f/ZrC composites fabricated by low-temperature liquid metal infiltration

Yulin Zhu[a], Song Wang[a,*], Hongmei Chen[a,b], Wei Li[a], Zhaohui Chen[a]

[a]*Science and Technology on Advanced Ceramic Fibers and Composites Laboratory, National University of Defense Technology, Deya Street, Changsha 410073, China*

[b]*Department of Mechanical Engineering, Hunan International Economics University, Changsha 410205, China*

Received 13 July 2013; received in revised form 9 October 2013; accepted 9 October 2013
Available online 18 October 2013

Abstract

Carbon fiber-reinforced zirconium carbide matrix (C_f/ZrC) composites were fabricated by a liquid metal infiltration process at 1200 °C, using low melting Zr_7Cu_{10}, ZrCu and Zr_2Cu alloys as infiltrators. The effects of Cu on microstructure and mechanical properties of the composites were investigated. The results indicated that the products were composed of either single- or polycrystalline ZrC, C and Cu. With increasing Cu content in the infiltrators, the yield of ZrC decreased from 43.7 vol% to 27.9 vol%. When ZrCu was used as an infiltrator, the obtained composites exhibited a better bending strength of 98.2 ± 3.1 MPa. What is more, the use of Zr_2Cu could provide the highest fracture toughness of the composites with a moderate debonding.

Keywords: B. Composites; B. Microstructure; C. Mechanical properties; D. Carbides; Liquid metal infiltration

1. Introduction

Zirconium carbide (ZrC) is usually referred to as an ultra-high temperature ceramic (UHTC) for its unique properties such as extremely high melting point, relatively low density, high strength [1–4], and superior ablation resistance at high temperatures [5,6], which enables it to be used in extreme environments associated with hypersonic flight and rocket propulsion [1,2,7]. However, the poor plasticity of ZrC ceramic restricts its development and applications [6,7]. A potentially effective approach to improve its toughness is introduction of long continuous carbon fibers into the ceramic as reinforcement [6–9].

Among the fabrication processes for continuous fiber reinforced ceramic matrix composites, the liquid metal infiltration (LMI) has many advantages, including short fabrication period, low cost, near net shape, etc. [10–13]. This process has been adopted to prepare C_f/ZrC composites, by infiltrating porous C_f/C preforms with molten Zr [6,9]. But due to the high melting point of Zr (1850 °C) [14], the infiltration process can only be operated above 1900 °C, resulting in a great damage to the fibers. Recently, Zr_2Cu alloy has been used as an infiltrator to produce C_f/ZrC composites at temperature as low as 1200 °C [7,15]. However, the effects of Cu additive on microstructure and performance of the final composites have not been reported so far.

In this paper, C_f/ZrC composites were prepared at relatively low temperature, by vacuum infiltrating porous C_f/C preforms with low melting Zr–Cu alloys. The influences of Cu content in the melts on microstructure and mechanical properties of the composites were investigated.

2. Experimental procedure

2.1. Materials preparation

Porous C/C preform with porosity of about 40% was fabricated by a needle-punching technique combined with the PIP method, using phenolic resins as the precursor. The carbon

*Corresponding author. Tel.: +86 731 84576441; fax: +86 731 84576578.
E-mail address: wangs_0731@163.com (S. Wang).

0272-8842/$ - see front matter © 2013 Elsevier Ltd and Techna Group S.r.l. All rights reserved.
http://dx.doi.org/10.1016/j.ceramint.2013.10.037

fiber (T300, an average diameter of about 7 μm, Toray in Japan) fraction is about 30 vol%.

Three Zr–Cu alloys with Zr/Cu molar ratios of 7:10, 1:1 and 2:1 were used as reactive infiltrators for this study. The alloy ingots were received from Hunan Rare Earth Metal & Material Institute, prepared with spongy Zr pieces (99.6% purity) and electrolytic Cu plates (99.99% purity) by arc melting.

The preparation of C_f/ZrC composites included stages as follows: Zr–Cu alloys were placed in graphite crucibles and heated up to 1200 °C in a vacuum of 0.5 Pa. After the alloys melted completely, C_f/C preforms were mechanically driven into the melts, kept there for 1–3 h, then separated from the liquid Zr–Cu baths and cooled spontaneously to room temperature.

2.2. Characterization

The volume fractions of solid phases and the theoretical porosities of the specimens were determined by inductively coupled plasma (ICP) and chemolysis, based on the theoretical densities of 6.63 g cm^{-3} for ZrC, 1.55 g cm^{-3} for deposited C, 8.96 g cm^{-3} for Cu, 6.49 g cm^{-3} for Zr and 1.76 g cm^{-3} for T300 fibers. The details were described elsewhere [7,16]. The open porosities were measured on five samples using the Archimedes method. The phases were analyzed by X-ray diffraction with a Bruker D8 Advance instrument. The microstructures were observed by scanning electronic microscopy (SEM, Quanta-200) and transmission electron microscopy (TEM; JEOL, Tokyo, Japan; JEM-2010F). The TEM sample was prepared by grinding a bulk sample to about 80 μm in thickness and then a 3 mm diameter disc was cut out. The disc was subsequently dimpled and ion milled.

2.3. Mechanical properties tests

Flexural strength and elastic modulus were measured using a four-point bending test (Model 5566, Instron Corp., High Wycombe, UK), according to GB/T 6569-2006 and GB/T 10700-2006 Standard (China), respectively. Length of the force arm was 15 mm and crosshead speed was 0.5 mm min^{-1}. At least 10 specimens with a dimension of 3.0 mm × 4.0 mm × 60 mm and a span of 45 mm were tested to obtain the average data. Fracture toughness was evaluated by the single-edged notched-beam test according to GB/T 23806-2009 Standard (China). Five samples with a span of 30 mm were measured at a crosshead speed of 0.05 mm min^{-1}. Length of the force arm was 15 mm. The test bars, 3.0 mm × 6.0 mm × 40 mm, were notched by electromachining with a 0.2 mm-diameter Mo line. The notches were about 0.2 mm in width and 3.0 mm in depth.

3. Results and discussion

3.1. Thermodynamics consideration

Assuming a complete consumption of Zr in the alloys, the reactions between carbon and Zr–Cu melts can be expressed as follows:

$$C(s)+\frac{1}{2}Zr_2Cu(l)\rightarrow ZrC(s)+\frac{1}{2}Cu(l) \quad (1)$$

$$C(s)+ZrCu(l)\rightarrow ZrC(s)+Cu(l) \quad (2)$$

$$C(s)+\frac{1}{7}Zr_7Cu_{10}(l)\rightarrow ZrC(s)+\frac{10}{7}Cu(l) \quad (3)$$

The changes of Gibbs free energy (ΔG°) were calculated to estimate the feasibility of the above reactions. The results (Fig. 1) show that ΔG° of all three reactions at temperature above 1200 K is negative. Thereby it is thermodynamically favorable to form ZrC phase from reactions between C and alloys. It is worth noting that ΔG° of reaction (3) is more negative than that of others, indicating that the formation of ZrC from Zr_7Cu_{10} is the most favorable. According to Zhang et al. [17], the increase of Cu could promote and accelerate Zr–C reaction occurrence by prior formation of liquids at a low temperature.

3.2. Composition and microstructure

XRD patterns of the obtained C_f/ZrC composites are shown in Fig. 2. It can be found that all the specimens have the same

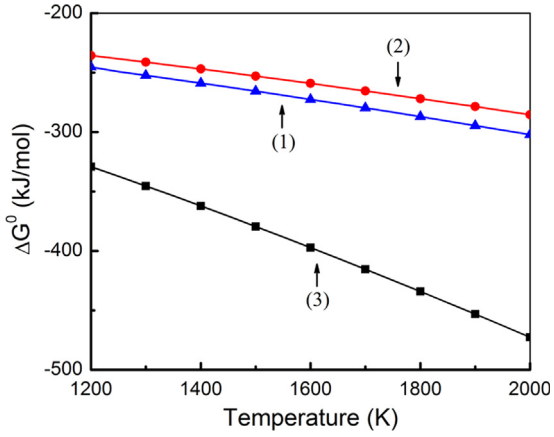

Fig. 1. Changes in Gibbs free energy for reactions (1)–(3).

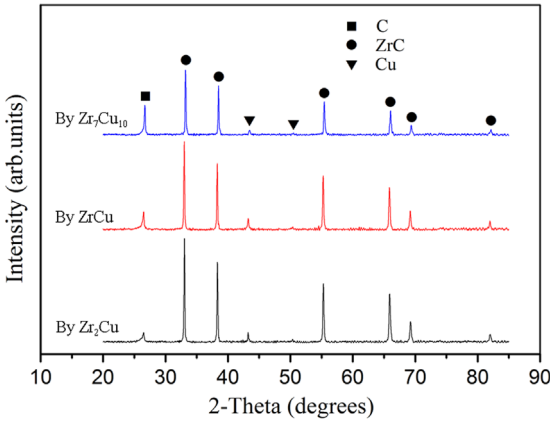

Fig. 2. XRD patterns of the C_f/ZrC composites fabricated by Zr–Cu alloys.

Table 1
Compositions of the C_f/ZrC composites fabricated by Zr–Cu alloys.

Specimens	Porosity (%)	Volume fractions of phases(vol%)				
		C-fiber	ZrC	C	Residual melt	
					Zr	Cu
By Zr_2Cu	9.9 ± 1.3	31.9 ± 2.7	43.7 ± 2.8	6.3 ± 1.4	1.7 ± 0.6	6.5 ± 1.2
By ZrCu	5.5 ± 0.7	31.9 ± 2.7	40.1 ± 2.1	8.3 ± 0.6	2.3 ± 1.1	11.9 ± 1.0
By Zr_7Cu_{10}	5.2 ± 0.9	31.9 ± 2.7	27.9 ± 1.7	15.8 ± 1.3	3.2 ± 1.4	16.0 ± 1.5

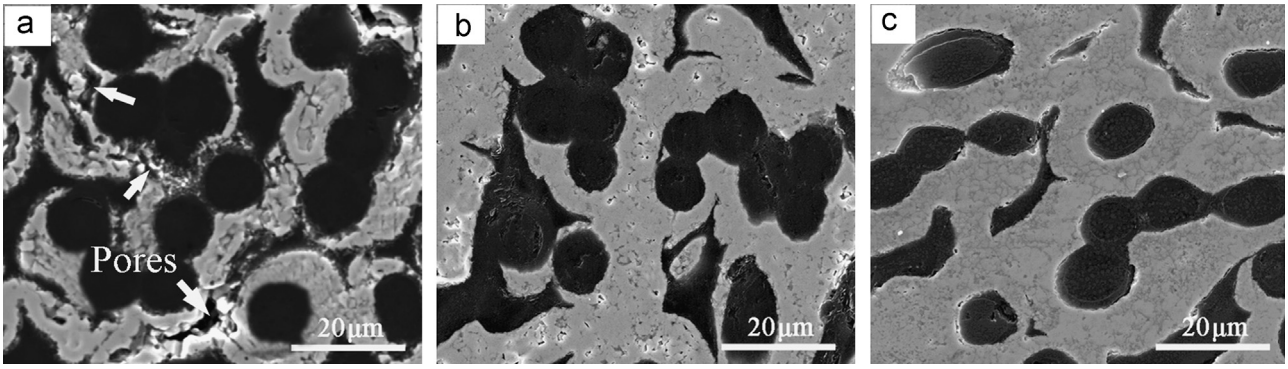

Fig. 3. SEM micrographs of cross-section of the C_f/ZrC composites fabricated by (a) Zr_2Cu, (b) ZrCu and (c) Zr_7Cu_{10}.

constituent phases ZrC, C and Cu. Therefore, the reaction products are in accordance with the predictions based on thermodynamic equilibrium. Cu instead of Zr_xCu_y compound as the product implies a complete consumption of Zr free from Cu/Zr ratio of the infiltrator. Table 1 presents the compositions of the C_f/ZrC composites. As indicated, ZrC with a yield of 27.9–43.7 vol% is demonstrated to be the dominant phase of the composites.

It is also revealed from Fig. 2 that, with increasing Cu in the alloys, the diffraction peaks of ZrC become weaker and the tiny peaks of carbon are enhanced. Confirmed by the results listed in Table 1, Cu exhibits a negative influence on production of ZrC. This can be ascribed to two aspects: one is that the increase of Cu would accordingly reduce the content of Zr, and then the formation of ZrC is limited due to lack of Zr supply. The other is that, based on the formation mechanism of ZrC reported previously [7,17] and the Cu–C phase diagram [18], the presence of Cu can depress the solubility of C in the melt and consequently inhibit the production of ZrC ceramics.

The representative cross-sections of the composites are shown in Fig. 3. As revealed, all the composites have relatively homogeneous distribution of phases. For the composites fabricated by Zr_2Cu, there exist many pores bigger than 1 μm (shown by arrows in Fig. 3a), meaning that the pores cannot be filled completely when Zr–Cu alloy with low Cu content is used as the infiltrator. On the contrary, the other two composites are much more compact (Fig. 3b and c). Therefore, it can be inferred that the increase of Cu favors densification of the C_f/ZrC composites. As reported by Adelsberg et al. [19] and Tong et al. [20], the growth of ZrC is rapid and expansive; thus the aperture necks are liable to be choked during the melt impregnation process, consequently retarding the next infiltration steps. Due to the repressive effect of Cu on Zr–C reaction, the increase of Cu in the melt can slow down the formation of ZrC to avoid aperture chokes.

The bright matrix parts were magnified to observe the details in Fig. 4. Either micrometer-sized or nano-sized particles with regular octahedron shapes are dispersed within the matrixes (Fig. 4a). Determined by TEM analysis, the micrometer scale particles are fundamental f.c.c. ZrC single crystals (Fig. 5a), and the nano-scale ones are polycrystalline (Fig. 5b). Their coexistence implies that the growth of ZrC is accompanied by a crystalline transformation from polycrystal to single crystal.

It can also be seen from Fig. 4 that, with increasing Cu in the alloys, both the size and crystallization of the grains decrease (Fig. 4b and c). That is, Cu inhibits the growth of ZrC. As reported in Refs. [21,22], the transition-metal carbides such as TiC or ZrC preferentially form non-stoichiometric TiC_x (ZrC_x) nuclei with a metastable crystallographic structure at the earlier period of nucleation, and then grow and evolve towards stoichiometric TiC (ZrC) with a stable lattice structure. It can be foreseen that the improvement of crystalline structure would be retarded consequentially with the increase of Cu in the melt. However, further studies are needed to confirm this.

3.3. Mechanical properties

Mechanical properties of the C_f/ZrC composites are summarized in Table 2. As indicated, the mechanical properties of

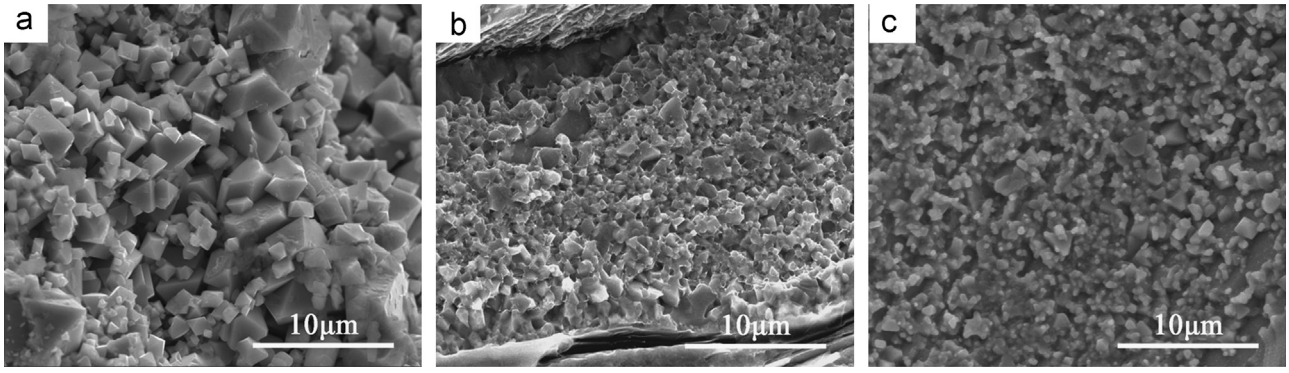

Fig. 4. SEM micrographs of the fracture surfaces focused on the matrixes of C_f/ZrC composites fabricated by (a) Zr_2Cu, (b) ZrCu and (c) Zr_7Cu_{10}.

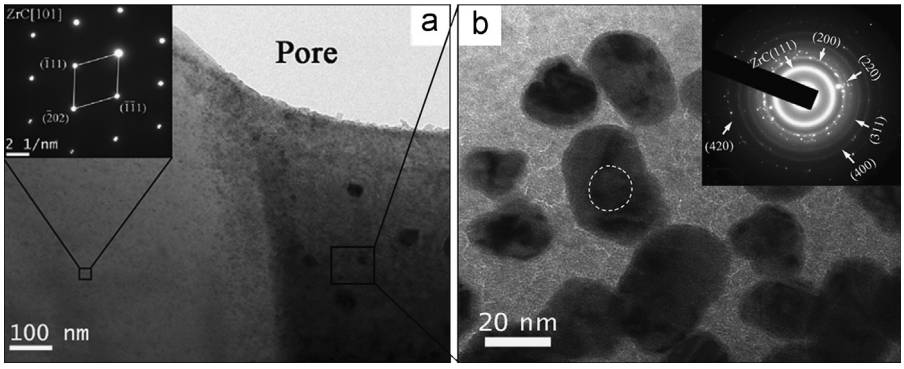

Fig. 5. TEM bright-field images of (a) the interface between a micrometer-sized ZrC particle and the residual melt with an inset of diffraction pattern from the particle, and (b) the residual Cu-enriched melt with an inset of diffraction pattern from the nano-sized pellet.

Table 2
Mechanical properties of the C_f/ZrC composites fabricated by Zr–Cu alloys.

Specimens	Flexural strength (MPa)	Elastic modulus (GPa)	Fracture toughness (MPa $m^{1/2}$)
By Zr_2Cu	62.7 ± 2.7	37.6 ± 1.9	6.3 ± 0.6
By ZrCu	98.2 ± 3.1	43.5 ± 2.8	5.5 ± 0.5
By Zr_7Cu_{10}	91.1 ± 3.4	49.8 ± 2.2	4.1 ± 0.8

the C_f/ZrC composites are apparently affected by Cu content in the alloy. The use of alloy with high Cu content could provide better bending strength and elastic modulus. For example, the composites fabricated by ZrCu have the highest flexural strength of 98.2 ± 3.1 MPa, about 50% higher than that of composites derived from Zr_2Cu. According to the above microstructure analysis the superior performance of composites from ZrCu might mainly benefit from their compact structure with high yield of ZrC, since the pores can greatly weaken the capacity of matrix to transfer load.

Typical bending load–displacement curves are shown in Fig. 6. For the curve of composites fabricated by Zr_7Cu_{10}, an initial quasi-linear elastic region is followed by an increasing nonlinear load up to a maximum. After reaching the maximum value the load decreases sharply, indicating that the sample displays a typical brittle fracture behavior. While for the curve

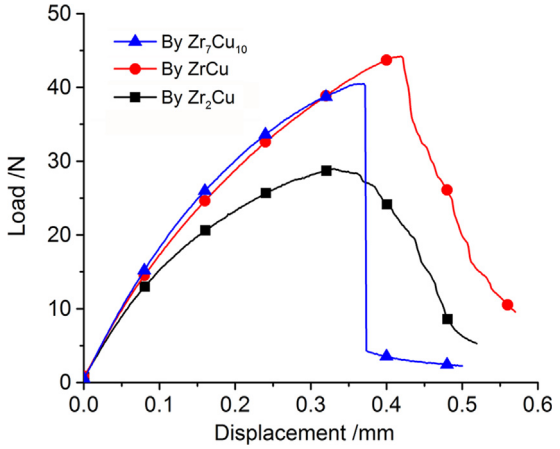

Fig. 6. Bending load/displacement curves of the C_f/ZrC composites fabricated by Zr–Cu alloys.

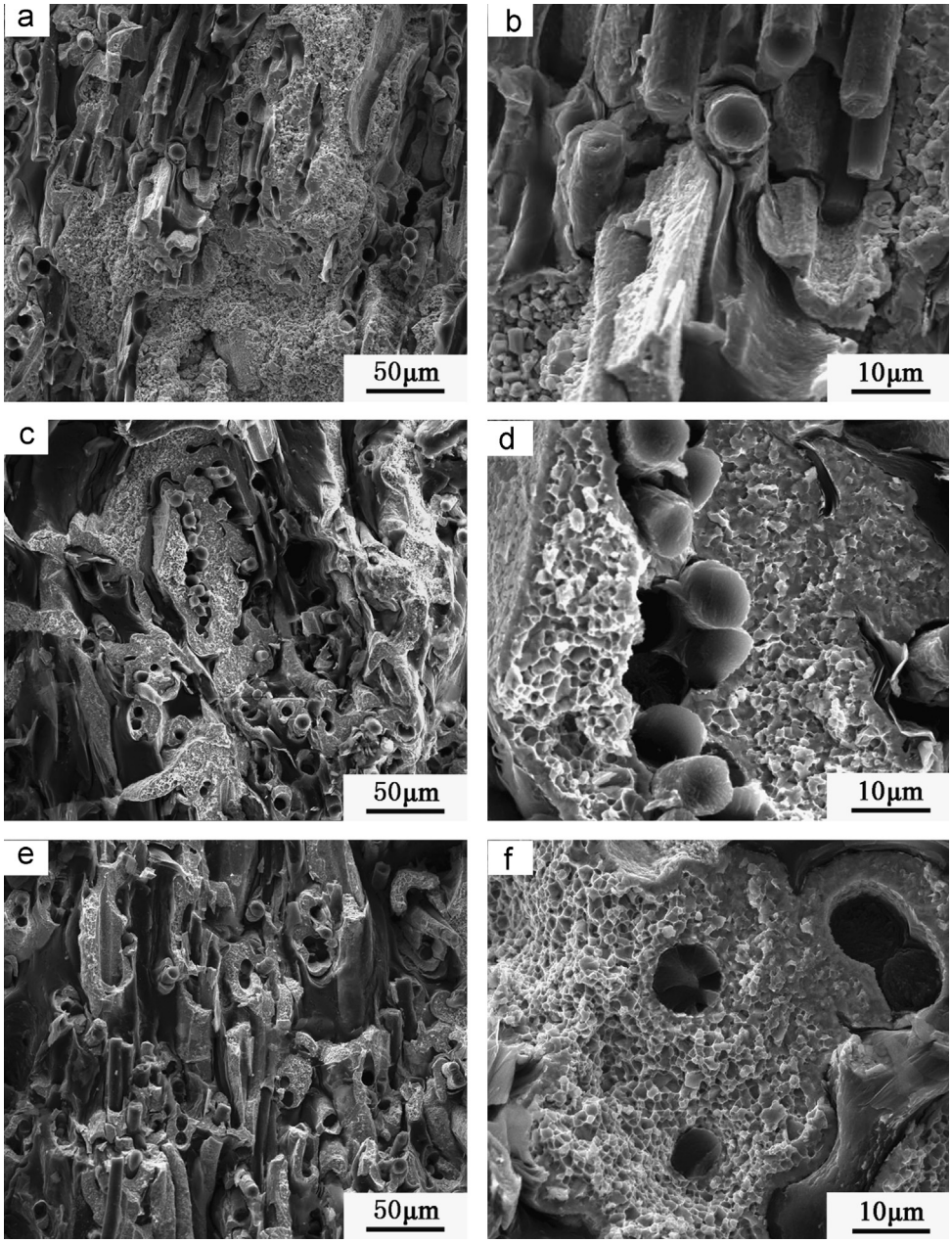

Fig. 7. SEM micrographs on the fracture surfaces of the C_f/ZrC composites fabricated by (a, b) Zr_2Cu alloys, (c, d) ZrCu, and (e, f) Zr_7Cu_{10}.

of sample fabricated by ZrCu, a zigzagging decline region can be observed. Particularly, the composites fabricated with Zr_2Cu show an evidently nonlinear rise until the maximum load is reached, and then a gradual decline follows. Therefore, the fracture behavior of the obtained composites is ameliorated with the decrease of Cu in the alloy, which is in agreement with the results listed in Table 2.

SEM photographs of the fracture surfaces are shown in Fig. 7. As revealed, there are fiber pullouts accompanied with the fracture process of the composites, though the pulled-out fibers are a few and short. Consistent with the evolution of fracture behavior, both the amount and length of pulled-out fibers decrease with increasing Cu in the alloys (Fig. 7b, d and f).

As discussed by Wang et al. [23], fiber/matrix interfacial characteristics play a crucial role in determining a toughening mechanism such as interfacial debonding and fiber pull-out. For the composites fabricated by Zr_2Cu, a strong ZrC-forming reaction might occur on the matrix/fiber interface. However, owing to the mismatch of thermal expansion coefficients (TEC) between C and ZrC ($TEC_C = 1.2$ ppm/K, $TEC_{ZrC} = 6.9$ ppm/K) [20], ZrC presents only a weak adherence to carbon fibers. During the damaging process, cracks from the matrix are deflected along the interfaces which favored the fibers pull-out (Fig. 7b) and contributed to relatively high fracture toughness. With increasing Cu content in the melt, the formation and growth of ZrC get slower and the mismatch of TEC is consequently alleviated. Besides, the residual

Cu-enriched melt acts as an excellent wetting agent to stick ZrC with fibers tightly. As a result, a strong-bonding interface is produced, facilitating cracks propagated straightly through the fibers and leading to a flat fracture surface (Fig. 7d and f).

4. Conclusions

The C_f/ZrC composites were fabricated at 1200 °C, by vacuum infiltrating porous C_f/C preforms with molten Zr_7Cu_{10}, ZrCu and Zr_2Cu alloys. The influences of Cu content in infiltrators on microstructure and mechanical properties of the C_f/ZrC composites were investigated. Results indicated that the obtained composites had the same constituent phases ZrC, C and Cu. ZrC as the dominant phase was identified to be either single- or polycrystalline. With the increase of Cu in infiltrators, both the growth and crystallization of ZrC grains were inhibited, and the yields of ZrC ceramic decreased from 43.7 vol% to 27.9 vol%. When ZrCu alloy was used as an infiltrator, the obtained composites have the highest strength of 98.2 ± 3.1 MPa. The use of Zr_2Cu could provide the highest fracture toughness of the composites with a moderate debonding.

Acknowledgments

This work was supported by National Natural Science Foundation of China (51002186 and 90916002) for financial support. The authors are grateful to Aid Program for Innovative Group of National University of Defense Technology and Aid Program for Science and Technology Innovative Research Team in Higher Educational Institutions of Hunan Province.

References

[1] S.M. Zhang, S. Wang, Y.L. Zhu, Z.H. Chen, Fabrication of ZrB_2–ZrC-based composites by reactive melt infiltration at relative low temperature, Scr. Mater. 65 (2011) 139–142.
[2] Q.G. Li, S.M. Dong, Z. Wang, P. He, H.J. Zhou, J.S. Yang, B. Wu, J.B. Hu, Fabrication and properties of 3-D C_f/SiC–ZrC composites, using ZrC precursor and polycarbosilane, J. Am. Ceram. Soc. 95 (2012) 1216–1219.
[3] D. Sciti, S. Guicciardi, M. Nygren, Spark plasma sintering and mechanical behaviour of ZrC-based composites, Scr. Mater. 59 (2008) 638–641.
[4] S.N. Karlsdottir, J.W. Halloran, Rapid oxidation characterization of ultra-high temperature ceramics, J. Am. Ceram. Soc. 90 (2007) 3233–3238.
[5] W. Sun, X. Xiong, B.Y. Huang, G.D. Li, H.B. Zhang, Z.K. Chen, X.L. Zheng, ZrC ablation protective coating for carbon/carbon composites, Carbon 47 (2009) 3368–3371.
[6] L.H. Zou, N. Wali, J.M. Yang, N.P. Bansal, Microstructural development of a C_f/ZrC composite manufactured by reactive melt infiltration, J. Eur. Ceram. Soc. 30 (2010) 1527–1535.
[7] Y.L. Zhu, S. Wang, W. Li, S.M. Zhang, Z.H. Chen, Preparation of carbon fiber-reinforced zirconium carbide matrix composites by reactive melt infiltration at relative low temperature, Scr. Mater. 67 (2012) 822–825.
[8] D. Zhao, C.R. Zhang, H.F. Hu, Y.D. Zhang, Ablation behavior and mechanism of 3D C/ZrC composite in oxyacetylene torch environment, Compos. Sci. Technol. 71 (2011) 1392–1396.
[9] Y.G. Wang, X.J. Zhu, L.T. Zhang, L.F. Cheng, Reaction kinetics and ablation properties of C/C–ZrC composites fabricated by reactive melt infiltration, Ceram. Int. 37 (2011) 1277–1283.
[10] W.B. Hillig, Melt infiltration approach to ceramic matrix composites, J. Am. Ceram. Soc. 71 (1988) C-96–C-99.
[11] S.M. Zhang, S. Wang, W. Li, Y.L. Zhu, Z.H. Chen, Microstructure and properties of W–ZrC composites prepared by the displacive compensation of porosity (DCP) method, J. Alloys Compd. 509 (2011) 8327–8332.
[12] D.W. Lipke, Y. Zhang, Y. Liu, B.C. Church, K.H. Sandhage, Near net-shape/net-dimension ZrC/W-based composites with complex geometries via rapid prototyping and displacive compensation of porosity, J. Eur. Ceram. Soc. 30 (2010) 2265–2277.
[13] J.N. Ness, T.F. Page, Microstructural evolution in reaction-bonded silicon carbide, J. Mater. Sci. 21 (1986) 1377–1397.
[14] W.M. Guo, J. Vleugels, G.J. Zhang, P.L. Wang, O.V. Biest, Effect of heating rate on densification, microstructure and strength of spark plasma sintered ZrB_2-based ceramics, Scr. Mater. 62 (2010) 802–805.
[15] D. Wang, Y.J. Wang, J.C. Rao, J.H. Ouyang, Y. Zhou, G.M. Song, Influence of reactive melt infiltration parameters on microstructure and properties of low temperature derived C_f/ZrC composites, Mater. Sci. Eng. A 568 (2013) 25–32.
[16] Y.L. Zhu, S. Wang, H.M. Chen, W. Li, J.M. Jiang, Z.H. Chen, Microstructure and mechanical properties of C_f/ZrC composites fabricated by reactive melt infiltration at relatively low temperature, Ceram. Int. 39 (2013) 9085–9089.
[17] M.X. Zhang, B. Huang, Q.D. Hu, J.G. Li, Study of formation behavior of ZrC in the Cu–Zr–C system during combustion synthesis, Int. J. Refract. Met. Hard Mater. 31 (2012) 230–235.
[18] H.R. Wang, Y.F. Ye, Z.Q. Shi, X.Y. Teng, G.H. Min, Crystallization processes in amorphous $Zr_{54}Cu_{46}$ alloy, J. Non-Cryst. Solids 311 (2002) 36–41.
[19] L.M. Adelsberg, L.H. Cadoff, J.M. Tobin, Kinetics of the zirconium–carbon reaction at temperatures above 2000 °C, Trans. Metall. Soc. AIME 236 (1966) 972–977.
[20] Y.G. Tong, S.X. Bai, K. Chen, C/C–ZrC composite prepared by chemical vapor infiltration combined with alloyed reactive melt infiltration, Ceram. Int. 38 (2012) 5723–5730.
[21] M.S. Song, M.W. Ran, Y.Y. Kong, In situ fabrication of ZrC powder obtained by self-propagating synthesis from Al–Zr–C elemental powders, Int. J. Refract. Met. Hard Mater. 29 (2011) 392–396.
[22] B. Cochepin, V. Gauthier, Crystal growth of TiC grains during SHS reactions, J. Cryst. Growth 304 (2007) 481–486.
[23] Z. Wang, S.M. Dong, Y.S. Ding, X.Y. Zhang, H.J. Zhou, J.S. Yang, B. Lu, Mechanical properties and microstructures of C_f/SiC–ZrC composites using T700SC carbon fibers as reinforcements, Ceram. Int. 37 (2011) 695–700.